Available online at www.sciencedirect.com
SCIENCE DIRECT®
Journal of Photochemistry and Photobiology A: Chemistry 172 (2005) 63–71
Journal of Photochemistry and Photobiology A:Chemistry
www.elsevier.com/locate/jphotochem

Dye sensitization of nanocrystalline TiO_2: enhanced efficiency of unsymmetrical versus symmetrical squaraine dyes

Saji Alex, U. Santhosh, Suresh Das*

Photosciences and Photonics Division, Regional Research Laboratory (CSIR), Trivandrum 695019, India

Received 7 June 2004; received in revised form 28 October 2004; accepted 12 November 2004
Available online 5 January 2005

Abstract

A series of novel symmetrical and unsymmetrical squaraine dyes have been synthesized and their comparative efficiencies as photosensitizers in dye sensitized solar cells (DSSCs) containing nanocrystalline TiO_2 photoelectrodes have been investigated. DSSCs employing unsymmetrical squaraines as sensitizers produced photocurrent with much higher efficiencies compared to DSSCs containing symmetrical squaraines. Aggregation of the dyes on the TiO_2 nanocrystalline electrode was observed to adversely affect the sensitization properties of symmetrical squaraines, whereas efficient sensitization was observed from both the monomeric and aggregated forms of the unsymmetrical squaraines.

Keywords: Dye sensitization; Solar cells; Squaraine dyes; Aggregation; Nanocrystalline TiO_2

1. Introduction

Dye sensitization of nanocrystalline semiconductors is an area, which continues to attract considerable attention since Graetzel first reported on the highly efficient ruthenium-complex sensitized nanocrystalline TiO_2-based dye sensitized solar cells (DSSCs) [1–7]. Among the various sensitizers investigated, polypyridyl complexes of ruthenium, such as N3 dye, *cis*-bis(isothiocyanato)bis(2,2′-bipyridyl-4,4′-dicarboxylate) ruthenium(II) [2] and the more recently reported 'black dye', tris(isothiocyanato)-2,2′,2″-terpyridyl-4,4′,4″-tricarboxylate ruthenium(II) (Fig. 1) have been reported to have solar energy to electricity conversion of up to 10.4% [6]. In contrast, although a wide variety of organic dyes have been investigated as sensitizers their performance in DSSCs has been reported to be very poor. Recently, Arakawa and co-workers have shown that certain coumarin and polyene based dyes can provide DSSCs with solar to electric power conversion of up to 7.7% [8,9]. It has also been shown that broad absorption can be obtained using a mixture of organic dyes, which do not interfere with the sensitization properties of each other [6,10]. These studies have led to renewed interest in the search for more efficient organic dye sensitizers for DSSCs.

Squaraines are a class of highly stable dyes, which have been extensively investigated for their sensitization properties [11,12]. They possess sharp and intense absorption bands in the visible and near infrared (NIR) regions and have been employed as sensitizers in a number of technological applications such as electrography [11], xerography [11] and optical data storage [13,14]. The ability of squaraine dyes to sensitize large band-gap semiconductors as well as their application as organic photovoltaic materials have been well investigated [15–22]. However, in view of the low efficiencies of sensitization of large band-gap semiconductors by squaraines [23,24], with few exceptions their use as sensitizers in DSSCs have not been well explored [19,25]. Most reported studies have utilized only symmetrical squaraines as sensitizers. We have synthesized a series of symmetrical and unsymmetrical squaraine dyes (Fig. 2) and their comparative efficiencies in DSSCs have been evaluated in order to

* Corresponding author. Tel.: +91 471 2515318; fax: +91 471 2490186.
E-mail address: sdaas@rediffmail.com (S. Das).

1010-6030/$ – see front matter © 2004 Elsevier B.V. All rights reserved.
doi:10.1016/j.jphotochem.2004.11.005

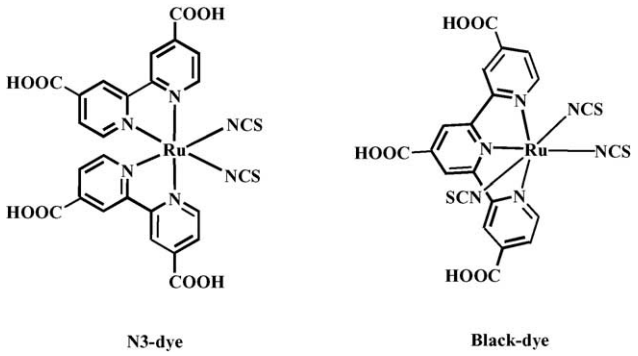

Fig. 1. Ruthenium polypyridyl complexes used as efficient sensitizers in DSSCs.

understand the factors that control light harvesting efficiency of these dyes. Here we report that the sensitization efficiencies of unsymmetrical squaraines in DSSCs are significantly higher than those of symmetrical squaraines. Molecular orbital calculations for these dyes indicated a unidirectional flow of electrons on excitation of unsymmetrical squaraines whereas increase in charge density towards the center of the molecule was observed for the symmetrical squaraines. These aspects as well as the role of dye aggregation on the electrode surface on the efficiency of squaraine sensitized DSSCs are discussed.

2. Experimental section

2.1. Reagents and materials

2-Methylbenzoselenazole, 2-methylbenzothiazole, lithium iodide (anhydrous) and *tert*-butylpyridine were purchased from Fluka. Squaric acid and 2,3,3-trimethylindolenine were obtained from Aldrich. The organic solvents employed were of spectroscopic grade and the chemicals used were analytical reagents of the highest available purity. N3 dye was synthesized and characterized according to an earlier reported procedure [26].

2.1.1. General synthesis of squaraine dyes ***Sq1*–*Sq7***

The symmetrical squaraine dye **Sq1** was synthesized using a reported procedure [27]. The symmetrical squaraine

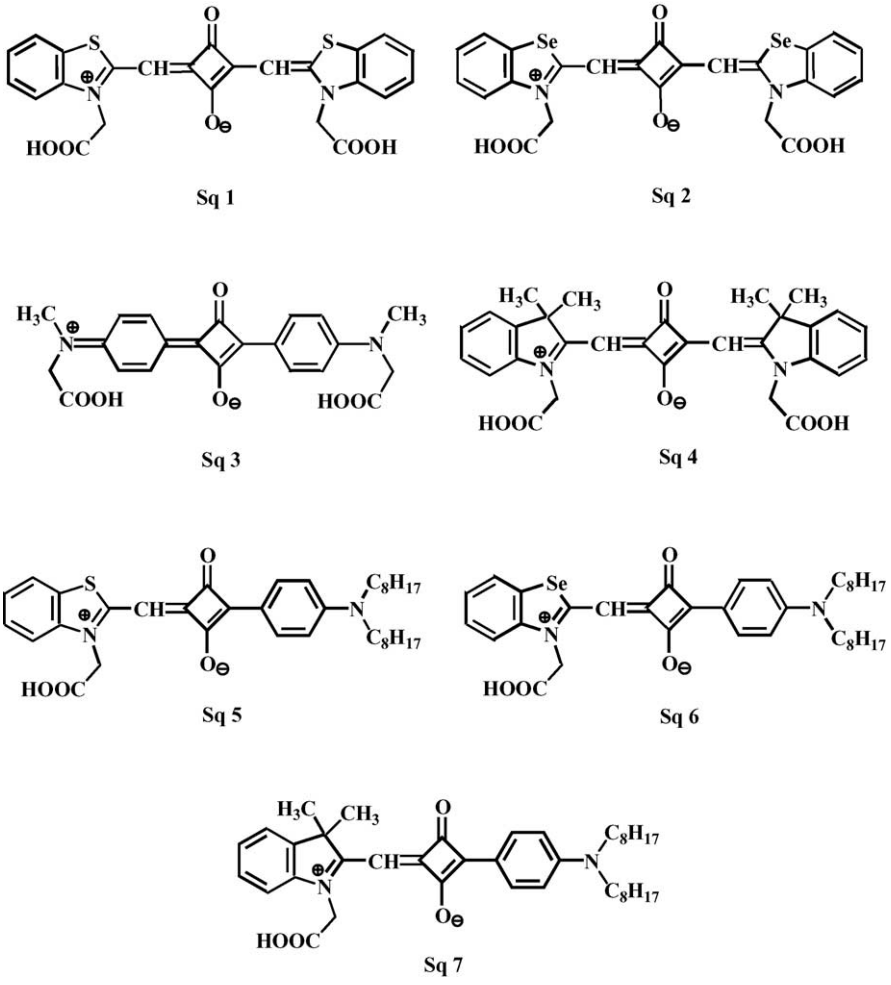

Fig. 2. Squaraine dyes used for the present study.

dyes **Sq2**–**Sq4** were synthesized using a similar procedure namely condensation of one equivalent of squaric acid with two equivalents of the respective nucleophiles under reflux in a solvent mixture of benzene and butanol (1:2) using a Dien-Stark condenser [27–31]. The unsymmetrical squaraine dyes **Sq5**–**Sq7** were synthesized by condensation of the semisquaric acid, 1-(4-*N*,*N*-dioctylaminophenyl)-2-hydroxycyclobuten-3,4-dione with one equivalent of the corresponding nucleophiles under reflux in a solvent mixture of benzene and butanol (1:2) using Dien-Stark condenser, adopting methods similar to those reported by Keil and Hartmann [32]. The dyes were purified by column chromatography on silica gel (100–200 mesh) by eluting with an appropriate solvent mixture of chloroform and methanol. All the dyes were characterized on the basis of analytical results and spectral data. All melting points were uncorrected and were determined on a Buchi melting point apparatus. IR spectra were recorded on a Shimadzu Prestige-21 FTIR-8400S IR spectrometer, ^{1}H NMR spectra were recorded on a Bruker–300 MHz NMR spectrometer and HRMS spectra where recorded on a JEOL JMS600 mass spectrometer.

- Bis[3-(carboxymethyl)benzothiazol-2-ylidene]squaraine (**Sq1**): yield 26%; mp 235 °C (decomp); IR (in KBr) 1734, 1658, 1565 cm^{-1}; ^{1}H NMR (DMSO-d$_6$) δ 7.87–7.23 (m, 8H), 5.67 (s, 2H), 5.12 (s, 4H); HRMS(FAB) *m*/*z* Calcd for $[M+1]^+$ 493.053; Found: 493.052.
- Bis[3-(carboxymethyl)benzoselenazol-2-ylidene]squaraine (**Sq2**): yield 15%; mp 244–246 °C; IR (in KBr) 1736, 1662, 1571 cm^{-1}; ^{1}H NMR (DMSO-d$_6$) δ 7.6–7.17 (m, 8H), 5.72 (s, 2H, CH), 4.96 (s, 4H); HRMS(FAB) *m*/*z* Calcd for $[M+1]^+$ 588.934; Found: 588.871.
- Bis[4-(*N*-carboxymethyl-*N*-methylamino)phenyl]squaraine (**Sq3**): yield 14%; mp 218–220 °C (decomp); IR (in KBr) 1741, 1620, 1596 cm^{-1}; ^{1}H NMR (CDCl$_3$) δ 8.26 (d, J = 9.3 Hz, 4H), 6.66 (d, J = 9.3 Hz, 4H), 5.66 (s, 4H), 3.99(s, 6H); HRMS(FAB) *m*/*z* Calcd for $[M]^+$ 408.132; Found: 408.211.
- Bis[1-carboxymehyl-2,3,3-trimethylindolenium-2-ylidene]squaraine (**Sq4**): yield 16%; mp 172–174 °C; IR (in KBr) 1743, 1582, 1521 cm^{-1}; ^{1}H NMR (DMSO-d$_6$) δ 7.6–7.17 (m, 8H), 5.72 (s, 2H), 4.96 (s, 4H); HRMS(FAB) *m*/*z* Calcd for $[M+1]^+$ 513.195; Found: 513.261.
- [3-(Carboxymethyl)benzothiazol-2-ylidene][4-(*N*,*N*-dioctylamino)phenyl]squaraine (**Sq5**): yield 23%; mp 215–216 °C; IR (in KBr) 1748, 1609, 1551 cm^{-1}; ^{1}H NMR (DMSO-d$_6$) δ 8.12 (d, J = 8.9 Hz, 2H), 7.70–7.39 (m, 4H), 6.65 (d, J = 8.9 Hz, 2H), 6.28 (s, 1H), 5.48 (s, 2H), 3.33 (t, 4H) 1.8–0.87 (m, 30H); HRMS(FAB) *m*/*z* Calcd for $[M+1]^+$ 603.328; Found: 603.341.
- [1-(Carboxymethyl)benzoselenazol-2-ylidene][4-(*N*,*N*-dioctylamino)phenyl]squaraine (**Sq6**): yield 14%; mp 228–230 °C; IR (in KBr) 1752, 1613, 1560 cm^{-1}; ^{1}H NMR (DMSO-d6) δ 8.13 (d, J = 9.3 Hz, 2H), 7.42–7.15 (m, 4H), 6.62 (d, J = 9.3 Hz, 2H), 6.39 (s, 1H), 4.98 (s, 2H), 3.39 (t, 4H) 1.8–0.88 (m, 30 H); HRMS(FAB) *m*/*z* Calcd for $[M]^+$ 650.262; Found: 650.276.
- [1-Carboxymehyl-2,3,3-trimethylindolenium-2-ylidene]-[4-(*N*,*N*-dioctylamino)phenyl] squaraine (**Sq7**): yield 15%; mp 148–150 °C; IR (in KBr) 1739, 1599, 1568 cm^{-1}; ^{1}H NMR (DMSO-d6) δ 8.03 (d, J = 8.9 Hz, 2H), 7.65-7.31 (m, 4H), 6.82 (d, J = 9.2 Hz, 2H), 5.87 (s, 1H), 5.21 (s, 2H), 3.45 (t, 4H) 1.6–0.87 (aliphatic, 36H); HRMS(FAB) *m*/*z* Calcd for $[M+2]^+$ 614.413; Found: 614.403.

All the dyes investigated in the present study, except **Sq3**, can potentially exist in their trans or *cis* isomeric forms. The *cis* isomers of this class of dyes which have been reported to be formed on photoexcitation of the trans isomers [33], are, however, unstable and decay back to trans isomer in the millisecond time domain.

2.1.2. Preparation of the nanocrystalline TiO_2 electrodes

A colloidal paste of TiO_2 was prepared from commercial TiO_2 powder (Degussa, P25) by following a reported procedure with slight modifications [2]. TiO_2 (6 g) was made into a paste by constant grinding in a porcelain mortar during slow addition of dilute aqueous acetic acid (10 mL). Finally 50 μL of Triton X-100 was added. Transparent conducting glass electrodes (F-doped SnO_2, <10 Ω/□, Hartford Glass Company, Germany) were cut into 1 cm × 1 cm size and were cleaned by sonicating for 20 min successively in a glass cleaning solution, in water and finally in ethanol and dried in a stream of nitrogen. The TiO_2 paste was coated on the conducting side of the electrode by screen-printing, allowed to dry in air following which it was sintered for 30 min at 450 °C. The film was then cooled slowly to a temperature of 80 °C, at which time it was immersed into 3.0×10^{-4} M solution of the dye in dry methanol kept at room temperature. The electrode was withdrawn from the solution after 12 h and washed with dry solvent to remove any physically adsorbed dye from the surface and then dried under a nitrogen atmosphere.

2.2. Photoelectrochemical measurements

The cell was assembled with the TiO_2-coated side of the electrode placed directly over a platinum coated counter electrode and the two electrodes were then clamped tightly using clips. A drop of electrolyte was then placed between the electrodes and allowed to wet the surfaces of the electrodes by capillary action. The electrolyte used was a solution of 0.5 M LiI and 0.05 M iodine in propylene carbonate–acetonitrile (v:v = 1:1) mixture. For preparation of the counter electrode, platinum was electroplated on the conducting side of a transparent conducting electrode from a 0.01 M solution of chloroplatinic acid in dilute HCl (1 M) using a 12 V source for 2 s.

For the photocurrent–photovoltage measurements, a 200 W mercury vapor lamp with a water IR filter and a 420 nm long pass UV filter served as a light source. The normal in-

tensity of incident light was 96 mW/cm^2. The photocurrent action spectra were measured using a 500 W Xenon lamp as a light source. A grating monochromator (SPEX Fluorolog) was introduced into the path of the excitation beam to produce monochromatic light. The number of incident photons was calculated by employing a power/energy meter calibrated using potassium oxalate actinometry at 352 nm. The current and voltage were measured using a Keithley Model 6517A electrometer. Action spectra were recorded by plotting monochromatic incident photon to current conversion efficiencies (IPCEs) against wavelength. IPCE, defined as the number of electrons injected by the excited dye in the external circuit divided by the number of incident photons, was obtained by recording the short-circuit photocurrents at various excitation wavelengths and using the following expression:

$$\text{IPCE}(\%) = \frac{1240 \times I_{sc}}{I_{inc} \times \lambda} \times 100 \quad (1)$$

where I_{sc} is the short-circuit photocurrent (A cm^{-2}), I_{inc} the incident light intensity in (W cm^{-2}) and λ is the excitation wavelength (nm).

The performance of DSSCs containing squaraine dyes as photosensitizers were compared with that of DSSCs containing N3 dye under the same experimental conditions. No special efforts were made to optimize for maximum possible efficiency. Photocurrent efficiencies were calculated without correcting for light absorption and reflection by the conducting glass support. All measurements were performed at room temperature.

2.3. Spectroscopy

Absorption measurements were made using a Shimadzu UV 3101PC UV–vis NIR spectrophotometer.

3. Results and discussion

3.1. Photophysical properties

The absorption spectra of the squaraine dyes investigated in the present study are shown in Fig. 3. Whereas the symmetrical squaraine dyes possess a sharp absorption band with maxima in the 630–670 nm range, the absorption spectra of the unsymmetrical squaraine dyes are broad and blue shifted (absorption maxima 600–630 nm) which is in accordance with the earlier reports [34].

Solvatochromic properties of squaraine dyes have been extensively investigated [15,31,34]. The absorption spectra of bis(dialkylaminophenyl) squaraines exhibit a weak bathochromic shift with increasing solvent polarity [34] and those of the methylene group containing symmetric squaraine dyes are virtually independent of solvent polarity [31]. MNDO and CNDO semi-empirical molecular orbital calculations have shown that excitation of symmetrical squaraines leads to an intramolecular charge transfer state with electrons being mainly transferred from the electron rich oxygen atoms to the electron deficient central cyclobutane ring [35]. The insensitivity of symmetric dyes to solvent polarity can, therefore, be attributed to charge-transfer on excitation being localized on the central C_4O_2 unit, which would result in very little solvent reorganization following the excitation process. In contrast, solvatochromic and molecular hyperpolarizability studies of unsymmetrical squaraine dyes have indicated that these dyes possess large dipole in the ground state compared to their excited state [15]. Table 1 shows the dependence of the absorption maxima of unsymmetrical squaraine dyes as well as that of two representative symmetrical squaraines (**Sq3** and **Sq4**) in common solvents. The hypsochromic shift with increasing solvent polarity for the unsymmetrical squaraine dyes in contrast to the slight bathochromic shift for the symmetrical squaraine dyes is clearly evident.

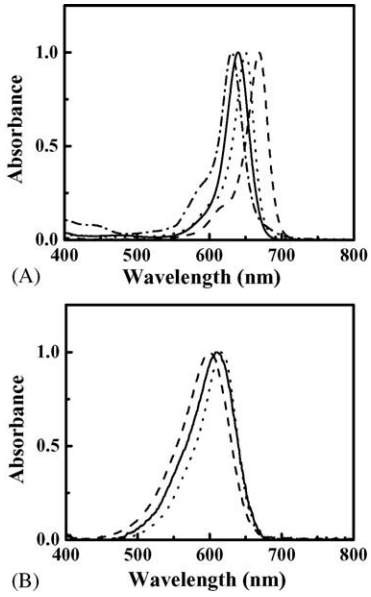

Fig. 3. Absorption spectra (normalized) of squaraine dyes in methanol: (A) symmetrical dyes, (···) **Sq1,** (- - -) **Sq2,** (—) **Sq3**, and (–·–·) **Sq4** and (B) unsymmetrical dyes, (- - -) **Sq5**, (—) **Sq6** and (···) **Sq7**.

Table 1
Solvatochromic properties of the squaraine dyes

Solvent	Absorption maxima (nm)				
	Sq3	**Sq4**	**Sq5**	**Sq6**	**Sq7**
Benzene	627	639	624	624	634
Toluene	625	638	619	624	633
Tetrahydrofuran	622	636	623	631	630
Acetonitrile	628	637	600	611	620
Dimethylformamide	650	643	607	614	619
Dimethylsulfoxide	652	647	605	619	624

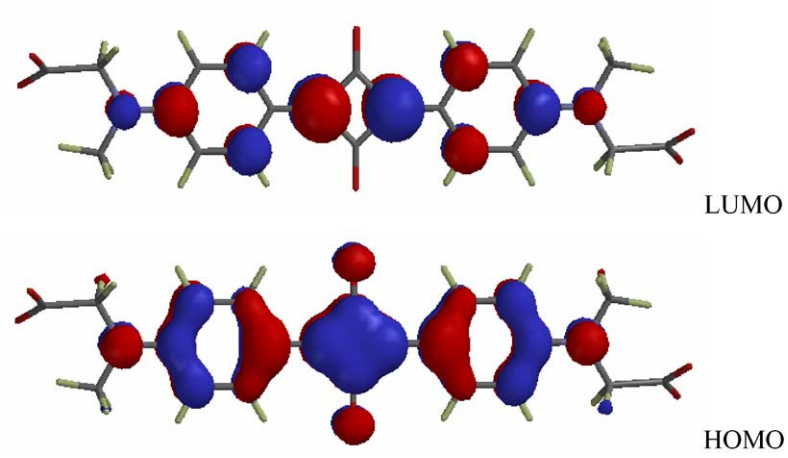

Fig. 4. Frontier MOs of the anionic form of the squaraine dye **Sq3**.

3.2. Electron density distribution of the frontier molecular orbitals

We have carried out molecular orbital calculations on the squaraine dyes using the Titan software package with a view to understanding the nature of electron distribution in the HOMO and LUMO states. Figs. 4–6 show the calculated molecular structure and the electron distribution of HOMO and LUMO of some of symmetrical and unsymmetrical squaraine dyes. The octyl groups attached to nitrogen have been replaced by methyl groups for ease of calculation and the carboxylate anionic form of the corresponding dyes were used for calculation since the dye will be bonded to the TiO_2 in the carboxylate form. Calculations for the symmetrical dye **Sq3** indicate that HOMO–LUMO excitation result in an increase in the electron density towards the center of the molecule in confirmation of the earlier studies [35]. Similar results were obtained for the methylene group containing symmetrical dye **Sq1**.

For the unsymmetrical squaraine dye **Sq5** however calculations indicated a clear shift of electron density from one end of the molecule to the other (Fig. 6). It is interesting to note that in the unsymmetrical squaraine dye the shift in electron density occurs towards the group linked through the methylene spacer, which also contains the carboxylic acid group used for linking the molecule to the semiconductor surface. Such a unidirectional flow of electron distribution can be expected to result in favorable charge separation and electron injection in DSSCs containing these dyes [36,37].

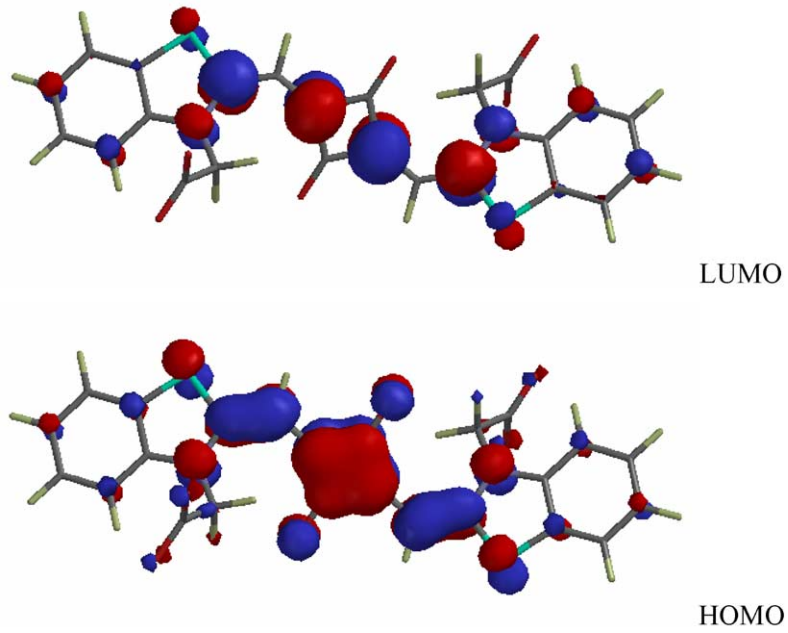

Fig. 5. Frontier MOs of the anionic form of the squaraine dye **Sq1**.

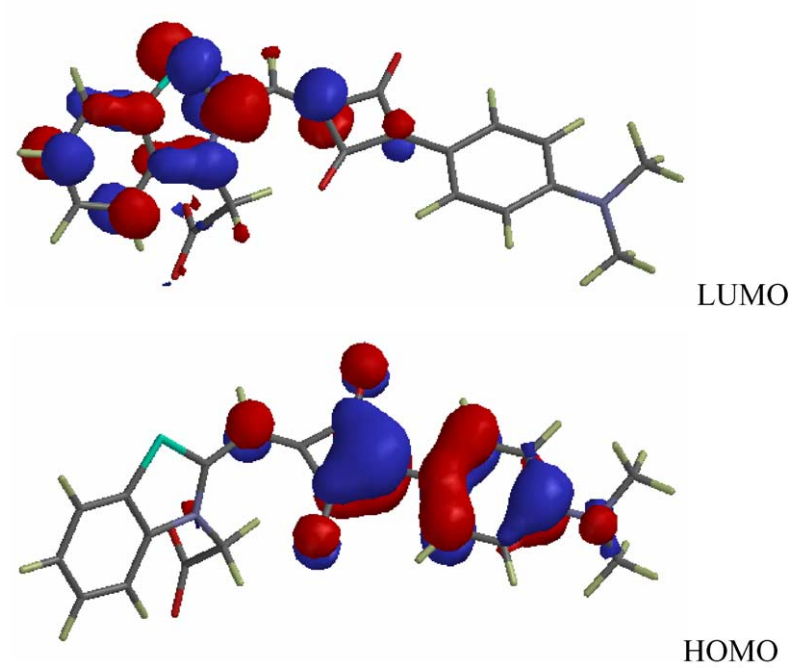

Fig. 6. Frontier MOs of the anionic form of the squaraine dye **Sq5**.

3.3. Photovoltaic properties of squaraine sensitized TiO_2 electrode

3.3.1. Photocurrent action spectra

The photocurrent action spectra of DSSCs containing nanocrystalline TiO_2 electrodes sensitized by squaraine dyes and iodine/iodide as the redox electrolyte were measured. The action spectra of the DSSCs sensitized by symmetrical and unsymmetrical squaraine dyes are shown in Figs. 7 and 8, respectively. It can be seen that all the DSSCs containing unsymmetrical squaraine dyes show significantly higher IPCE values compared to those containing symmetrical squaraine dyes.

The action spectrum of a DSSC is expected to resemble the absorption spectrum of the sensitizing dye, since the photocurrent is generated by the injection of electrons from the adsorbed excited dye molecules into the conduction band of the large band gap semiconductor. The action spectra of the DSSCs employing symmetrical squaraine dyes, **Sq1**, **Sq2**, and **Sq3** are, however, much broader compared to the solution state absorption spectra, which could be attributed to aggregation of the dyes on the TiO_2 surface. Since the dye is strongly bonded to the TiO_2 surface its extraction using solvents was not possible. The reflectance spectrum of a film of **Sq2** deposited on a plain glass plate (Fig. 9), indicates a broad

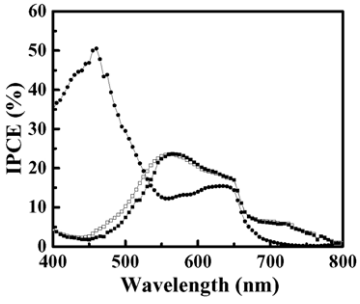

Fig. 8. Action spectra of TiO_2-based DSSCs employing unsymmetrical squaraine dyes as sensitizers: (□) **Sq5**, (■) **Sq6**, and (●) **Sq7**.

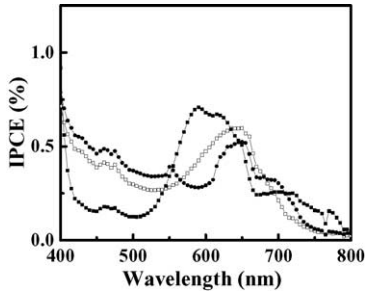

Fig. 7. Action spectra of TiO_2-based DSSCs employing symmetrical squaraine dyes as sensitizers: (□) **Sq1**, (■) **Sq2**, and (●) **Sq3**.

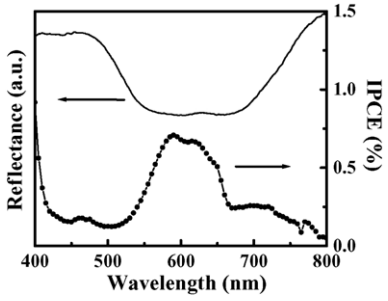

Fig. 9. The solid-state reflection spectrum and action spectrum of the DSSC employing **Sq2**.

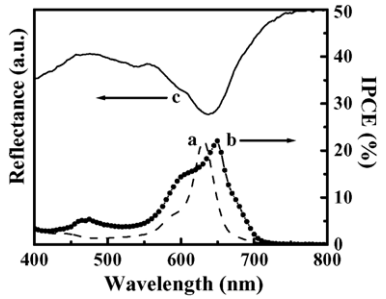

Fig. 10. (a) Absorption spectrum of **Sq4** in methanol, (b) action spectrum of the DSSC employing **Sq4** and (c) its solid-state reflection spectrum.

absorption band which closely matches the action spectrum of the DSSC. Redissolution of these films in methanol gave back the original spectra of the dye confirming that broadening of the absorption band is due to aggregation and not due to degradation of the dye. Similar broadening of absorption and low IPCE values were obtained for DSSCs containing the symmetrical squaraines **Sq1** and **Sq3**.

The photosensitization behavior of the symmetrical squaraine dye **Sq4** was however significantly different from that of the other symmetrical squaraine dyes. Fig. 10 shows the photocurrent action spectrum as well as the reflection spectrum of a thin film of **Sq4** on glass. The absorption spectrum of the dye dissolved in methanol is also included for comparison. The relatively sharp nature of the photocurrent action and reflectance spectra indicates that the tendency for **Sq4** to form aggregates is much lesser than that for the other symmetrical dyes. This may be attributed to the steric hindrance caused by the presence of the methyl groups in the indolenium moiety. The higher value of IPCE for **Sq4** compared to that for the other symmetrical squaraines indicates that aggregation has a significantly detrimental effect on the ability of the dyes **Sq1**–**Sq3** to sensitize TiO_2.

The photocurrent action spectra as well as the reflectance spectra of the unsymmetrical squaraine dye **Sq6** is shown in Fig. 11. In addition to the peak around 650 nm, an intense peak is clearly visible around 500 nm both in the action and reflectance spectra. The long wavelength band closely matches the absorption spectrum of the dye in solution. As in the case of the symmetrical dyes, redissolution of the dye film into solution gave back its original spectrum ruling out degradation of the dye being responsible for the appearance of the short wavelength band. The short wavelength band may, therefore, be attributed to formation of aggregated species. Kim et al. have earlier reported that some squaraine surfactants form blue-shifted H-aggregates on SnO_2 surfaces absorbing in the 500 nm region [21]. The photocurrent action and reflection spectra of **Sq5** and **Sq7** also exhibit both the monomer and blue shifted aggregate bands.

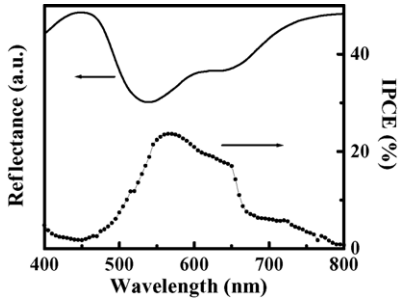

Fig. 11. The solid-state reflection spectrum of **Sq6** and action spectrum of the DSSC employing **Sq6**.

3.4. Aggregation properties of unsymmetrical squaraine dyes in methanol–water mixture

In order to confirm the blue-shifted absorption observed in the films of the unsymmetrical squaraine dyes arise due to formation of aggregates, their aggregation behavior was investigated in methanol–water solvent mixtures. Fig. 12 shows the changes in the absorption spectra of **Sq5** in 50% water–methanol with increasing concentration of the dye.

At lower concentrations, the absorption maximum is centered on 596 nm. With increasing concentration the absorption around 511 nm increases in intensity and this becomes the predominant peak at higher dye concentrations. The 511 nm band formed at higher dye concentrations can be attributed to formation of H-type aggregates. Similar observations were made for **Sq6** and **Sq7**.The monomer–aggregate equilibrium for these dyes could be shifted in favor of the monomer either by increasing the concentration of methanol in the solvent mixture or by increasing the temperature of the solution. Fig. 13 shows the effect of temperature on the absorption spectra of the dye **Sq5** in 50% water–methanol solvent mixture.

With increasing temperature the peak corresponding to the aggregate decreases and a corresponding increase in the monomer absorption is observed. The observed change was fully reversible on cooling the solution. These results confirm that blue shifted band observed in the reflectance and photocurrent action spectra arise due to formation of dye aggregates in the films.

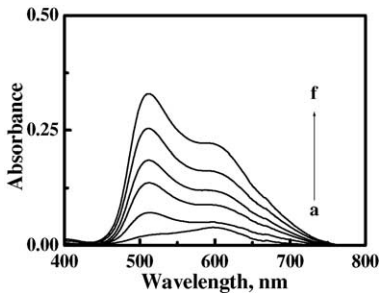

Fig. 12. Concentration effect of **Sq5** in 50% water–methanol (a) 0.7×10^{-6} mol dm^{-3}, (b) 2.1×10^{-6} mol dm^{-3}, (c) 4.3×10^{-6} mol dm^{-3}, (d) 5.5×10^{-6} mol dm^{-3}, (e) 7.2×10^{-6} mol dm^{-3}, and (f) 8.9×10^{-6} mol dm^{-3}.

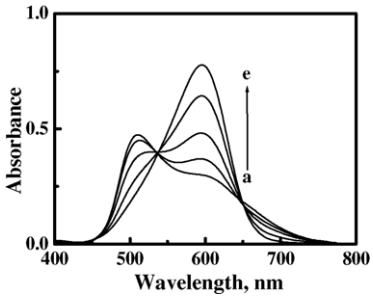

Fig. 13. Effect of temperature on the absorption spectra of the dye **Sq5** (10.3×10^{-6} mol dm^{-3}) in 50% water–methanol solvent mixture (a) 25°C, (b) 35°C, (c) 55°C, (d) 65°C, and (e) 70 °C.

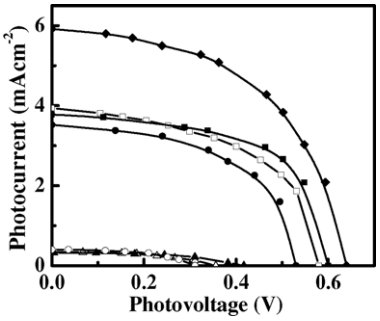

Fig. 14. Photocurrent–voltage curves of the DSSCs based on squaraine dyes sensitized nanocrystallineTiO_2: (△) **Sq1**, (▲) **Sq2**, (◯) **Sq3**, (●) **Sq4**, (□) **Sq5**, (■) **Sq6**, (♦) **Sq7**.

3.5. Current voltage characteristics

The power output features of the cells were evaluated by recording photovoltage and photocurrent at different load resistances. Fig. 14 shows the current–voltage characteristics obtained with DSSCs based on squaraine-sensitized nanocrystalline TiO_2 electrodes.

The photoelectrochemical parameters evaluated from the curves in Fig. 14 for various electrodes are summarized in Table 2. The value obtained for a DSSC using a N3 dye coated TiO_2 electrode under the same experimental conditions is also included in Table 2 for comparison. It can be seen that the photoelectric conversion data for DSSCs containing unsymmetrical squaraine dyes are superior to those obtained with symmetrical squaraine dyes. The only exception among the symmetrical squaraine dyes is for DSSCs containing **Sq4** which has similar output power characteristics to the DSSCs containing unsymmetrical dyes.

Table 2
Photoelectrochemical parameters of the dye sensitized solar cells employing squaraine dyes

Dye	V_{oc} (V)	I_{sc} (mAcm^{-2})	FF (%)	Efficiency (%)
Sq1	0.36	0.34	46.2	0.06
Sq2	0.42	0.32	51.6	0.07
Sq3	0.31	0.40	53.2	0.07
Sq4	0.53	3.52	53.4	1.04
Sq5	0.58	3.94	52.5	1.25
Sq6	0.60	3.78	60.5	1.43
Sq7	0.64	5.92	52.6	2.08
N3	0.64	10.08	59.3	3.98

Conditions: incident light, 200 W-mercury vapor lamp 96 mW cm^{-2}; electrolyte, 0.5 M LiI, 0.05 M I_2 and 1 M 4-*tert*-butylpyridine in propylenecarbonate–acetonitrile (v:v = 1:1) mixture; area of cells, 0.3 cm^2.

4. Conclusions

A series of symmetrical and unsymmetrical squaraine dyes have been synthesized and their photocurrent generating efficiencies in DSSCs were evaluated. Aggregation of symmetrical dyes on the TiO_2 photoelectrode results in significant decrease in their sensitization efficiency, whereas efficient sensitization was observed from both the monomeric and aggregated forms of the unsymmetrical squaraines. Molecular orbital calculations showed a unidirectional flow of electrons on excitation of unsymmetrical squaraines, as opposed to flow of electron towards the center of the molecule on excitation of symmetrical squaraines, which could result in improved charge separation from the excited state of the symmetrical squaraines.

Acknowledgments

We would like to thank the Department of Science and Technology, Council of Scientific and Industrial Research (COR 0003), Government of India for financial support. This is contribution No. RRLT-PPD-185 from Regional Research Laboratory, Trivandrum.

References

[1] B. O'Regan, M. Graetzel, Nature 353 (1991) 737.
[2] M.K. Nazeeruddin, A. Kay, I. Rodicio, R. Humphry-Baker, E. Muller, P. Liska, N. Vlachopoulos, M. Graetzel, J. Am. Chem. Soc. 115 (1993) 6382.
[3] M.K. Nazeeruddin, P. Pechy, T. Ronouard, S.M. Zakeeruddin, R. Humphry-Baker, P. Comte, P. Liska, L. Cevey, E. Costa, V. Shklover, L. Spiccia, G.B. Deacon, C.A. Bignozzi, M. Graetzel, J. Am. Chem. Soc. 123 (2001) 1613.
[4] A. Hagfeldt, M. Graetzel, Chem. Rev. 95 (1995) 49.
[5] A. Hagfeldt, M. Graetzel, Acc. Chem. Res. 33 (2000) 269.
[6] M. Graetzel, J. Photochem. Photobiol. C: Photochem. Rev. 4 (2003) 145.
[7] M. Graetzel, Nature 414 (2001) 338.
[8] K. Hara, K. Sayama, Y. Ohga, A. Shinpo, S. Suga, H. Arakawa, Chem. Commun. (2001) 569.
[9] K. Hara, M. Kurashigo, Y. Dan-oh, C. Kasasa, Y. Ohga, A. Shinpo, S. Suga, K. Sayama, H. Arakawa, New. J. Chem. 27 (2003) 783.
[10] P.M. Jayaweera, S.S. Palayangoda, K. Tennakone, J. Photochem. Photobiol. A: Chem. 140 (2001) 173.
[11] K.-Y. Law, Chem. Rev. 93 (1993) 449.

[12] S. Das, K.G. Thomas, M.V. George, in: V. Ramamurthy, K.S. Schanze (Eds.), Molecular and Supramolecular Photochemistry: Organic Photochemistry, vol. 1, 1997, p. 467.
[13] R.O. Loutfy, C.K. Hsiao, P.M. Kazmaier, Photogr. Sci. Eng. 27 (1983) 5.
[14] M. Matsuoka, in: M. Matsuoka (Ed.), Infrared Absorbing Dyes, Plenum Press, New York, 1990, p. 19.
[15] C.-T. Chen, S.R. Marder, L.-T. Cheng, J. Am. Chem. Soc. 116 (1994) 3117.
[16] S. Hotchandani, S. Das, K.G. Thomas, M.V. George, P.V. Kamat, Res. Chem. Intermed. 20 (1994) 927.
[17] C. Nasr, S. Hotchandani, P.V. Kamat, S. Das, K.G. Thomas, M.V. George, Langmuir 11 (1995) 1777.
[18] P.V. Kamat, S. Hotchandani, M. de Lind, K.G. Thomas, S. Das, M.V. George, J. Chem. Soc. Faraday Trans. 89 (1993) 2397.
[19] W. Zhao, Y.J. Hou, X.S. Wang, B.W. Zhang, Y. Cao, R. Yang, W.B. Wang, X.R. Xiao, Sol. Energy Mater. Sol. Cells 58 (1999) 173.
[20] M.J. Paterson, L. Blancafort, S. Wilsey, M.A. Robb, J. Phys. Chem. A 106 (2002) 11431.
[21] Y.-S. Kim, K. Liang, K.-Y. Law, D.G. Whitten, J. Phys. Chem. 98 (1994) 984.
[22] A.P. Piechowski, G.R. Bird, D.L. Morel, E.L. Stogryn, J. Phys. Chem. 88 (1984) 934.
[23] P.V. Kamat, S. Das, K.G. Thomas, M.V. George, Chem. Phys. Lett. 178 (1991) 75.
[24] N. Takeda, B.A. Parkinson, J. Am. Chem. Soc. 125 (2003) 5559.
[25] K. Sayama, S. Tsukagoshi, T. Mori, K. Hara, Y. Ohga, A. Shinpo, Y. Abe, S. Suga, H. Arakawa, Sol. Energy Mater. Sol. Cells 80 (2003) 47.
[26] M.K. Nazeeruddin, S.M. Zakeeruddin, R. Humphry-Baker, M. Jirousek, P. Liska, N. Vlachopoulos, V. Shklover, C.H. Fischer, M. Graetzel, Inorg. Chem. 38 (1999) 6298.
[27] S. Das, K.G. Thomas, K.J. Thomas, V. Madhavan, D. Liu, P.V. Kamat, M.V. George, J. Phys. Chem. 100 (1996) 17310.
[28] H.-E. Sprenger, W. Ziegenbein, Angew. Chem. Int. Ed. Engl. 6 (1967) 553.
[29] A.H. Schmidt, Synthesis (1980) 961.
[30] S. Das, K. George Thomas, R. Ramanathan, P.V. Kamat, M.V. George, J. Phys. Chem. 97 (1993) 13625.
[31] S. Das, K.G. Thomas, K.J. Thomas, M.V. George, P.V. Kamat, J. Phys. Chem. 98 (1994) 9291.
[32] D. Keil, H. Hartmann, Dyes Pigm. 49 (2001) 161.
[33] A.S. Tatikolov, S.M.B. Costa, J. Photochem. Photobiol. A: Chem. 140 (2001) 147.
[34] K.-Y. Law, J. Phys. Chem. 99 (1995) 9818.
[35] R.W. Bigelow, H.-J. Freund, Chem. Phys. 107 (1986) 159.
[36] K. Hara, T. Sato, R. Katoh, A. Furube, Y. Ohga, A. Shinpo, S. Suga, K. Sayama, H. Sugihara, H. Arakawa, J. Phys. Chem. B 107 (2003) 597.
[37] N.J. Cherepy, G.P. Smestad, M. Graetzel, J.Z. Zhang, J. Phys. Chem. B 101 (1997) 9342.